Available online at www.sciencedirect.com
SCIENCE DIRECT®
Journal of Fluorine Chemistry 120 (2003) 143–150
JOURNAL OF FLUORINE CHEMISTRY
www.elsevier.com/locate/jfluchem

A study on the formation mechanism of graphite fluorides by Raman spectroscopy

Vinay Gupta[a], Tsuyoshi Nakajima[a,*], Yoshimi Ohzawa[a], Boris Žemva[b]

[a]*Department of Applied Chemistry, Aichi Institute of Technology, Yakusa-cho, Toyota-shi 470-0392, Japan*
[b]*Jožef Stefan Institute, Jamova 39, 1000 Ljubljana, Slovenia*

Received 1 August 2002; received in revised form 7 November 2002; accepted 11 November 2002

Abstract

Raman spectra were measured of highly fluorinated graphite samples prepared at room temperature, 380 and 515 °C. C_xF prepared at room temperature showed a novel downshifted band at 1555–1542 cm^{-1} along with G band at 1593–1583 cm^{-1}. Similar behavior is also observed for samples prepared at 380 and 515 °C at early stages of fluorination, after which the Raman shifts completely disappeared. Raman spectra as well as X-ray diffraction (XRD) analysis suggest that graphite fluorides, $(CF)_n$ and $(C_2F)_n$ are formed via fluorine-intercalated phase with planar graphene layers.

Keywords: Graphite fluoride; Fluorine–graphite intercalation compound; Raman spectroscopy

1. Introduction

Graphite fluoride $(CF)_n$ was first synthesized by Ruff and Bretschneider by the reaction of elemental fluorine with graphite at 420 °C [1]. Later Kita et al. [3] discovered another form of graphite fluoride known as dicarbon monofluoride $(C_2F)_n$. Both types of fluorides are formed at high temperatures and have unique physicochemical properties [1–6]. The $(C_2F)_n$ is formed between 350 and 400 °C from highly crystalline graphite whereas $(CF)_n$ is prepared from various kinds of carbon materials [4,5]. Both fluorides are insulator due to covalent C–F bonding with sp^3 type. The $(C_2F)_n$ is black in color whereas $(CF)_n$ shows a wide range of colors from gray to white [4,5]. It is an excellent lubricant and has high electrochemical performance in primary lithium battery [4,5]. Graphite also reacts with fluorine at room temperature to form fluorine–graphite intercalation compound C_xF [4–23]. However, the reaction requires the presence of a Lewis acid such as HF. Fluorine can easily accept electron from graphite in the presence of a fluoride such as HF to form mobile HF_2^- anions and is easily intercalated between graphene layers [5–13]. C_xF is black in color and an electrical conductor. The nature of C–F bond in C_xF is ionic to semi-covalent with increasing concentration of fluorine between graphene layers. Purely ionic C_xF compounds are unstable even at ambient temperature and in high vacuum [11,13,15]. On the other hand, semi-covalent C_xF starts to decompose at a high temperature [12].

Among known vibration modes of graphite, E_{2g} modes are Raman active as fundamental. One is shear type rigid mode at 42 cm^{-1} (E_{2g1}) and the other is in plane stretching mode at 1580 cm^{-1} (E_{2g2}) often called as G mode. In case of polycrystalline graphite, another mode at 1350 cm^{-1} designated as D mode appears, being attributed to the disorder induced A_{1g} mode [16–18]. The intensity of A_{1g} mode is inversely proportional to the effective crystallite size L_a [16,17]. The Raman spectroscopic studies to characterize C_xF samples were performed by Mallouk et al. [19] for stage 1 $C_xF_{1-\delta}(HF)_\delta$ ($2 \leq x \leq 5$), Rao et al. [20,21] for C_xF samples ($2.9 \leq x \leq 7.8$) prepared from vapor-grown graphite fiber and by Ohana et al. [22] for $C_{12}F$ and $C_{6.4}F$ obtained from highly oriented pyrolytic graphite (HOPG). These studies showed that the Raman shift at 1580 cm^{-1} moves to 1615 cm^{-1} by the formation of ionic C_xF at room temperature. This upshifted phonon mode gradually moves to the lower Raman shift with increasing intercalated fluorine [19–24]. Change in the C–F bond length from the ionic

* Corresponding author. Tel.: +81-565-48-8121x2201; fax: +81-565-48-0076.
E-mail addresses: vinay@ac.aitech.ac.jp (V. Gupta), nakajima@ac.aitech.ac.jp (T. Nakajima).

0022-1139/02/$ – see front matter
doi:10.1016/S0022-1139(02)00323-8

Table 1
X-ray diffraction data and composition of C_xF samples prepared with K_2NiF_6 or $KAgF_4$ and elemental fluorine at room temperature

Sample	F_2 ($\times 10^5$ Pa)	Fluoride	X-ray diffraction data			Composition
			Stage[a]	I_c (nm)	a_0 (nm)	
R-1	7.9	K_2NiF_6	1 (2) (3)	0.6435 (0.9334) (1.231)	0.2464	$C_{1.88}F(HF)_{0.58}$
R-2	11.8	K_2NiF_6	1	0.6467	0.2466	$C_{1.64}F$
R-3	11.8	K_2NiF_6	1 (2) (3)	0.6388 (0.9418) (1.240)	0.2466	$C_{1.46}F(HF)_{0.35}$
R-4	11.8	$KAgF_4$	1	0.6281	0.2477	$C_{1.37}F$
R-5	11.8	$KAgF_4$	1	0.6259	0.2473	$C_{1.25}F$

[a] The values in parentheses represent minor phases.

for stage 2 and higher stage C_xF to the semi-covalent for stage 1 C_xF is responsible for this unique feature. For stage 2 and higher, the C–C bond length shrinks by an electron transfer from graphite to intercalated fluorine. As a result the vibration energy of graphene layer increases. However, the C–C bond length in graphene layer is increased by the formation of stage 1 C_xF with a composition of C_4F to $C_{1.3}F$ [6,19–24], which implies that the vibration energy of graphene layer decreases with increasing fluorine content at stage 1. The upshifted peak moves back to the original position of 1580 cm^{-1} at C_2F. This peculiar behavior is only observed for fluorine-intercalated graphite. This anomalous shift can be explained in terms of a decrease in the hole concentration in the graphene layers with increasing fluorine concentration, i.e. an increase in C–C bond length in the graphene layer. In this paper, a study on Raman spectra of highly fluorinated graphites prepared at room and high temperatures is reported to show the formation mechanism of graphite fluoride at high temperatures.

2. Results and discussion

2.1. Composition, structure and nature of C–F bonding of highly fluorinated graphite samples

The fluorination conditions and composition of the highly fluorinated graphite samples are given in Tables 1–3 [23–25]. Table 1 represents typical examples of reaction conditions, X-ray diffraction (XRD) data and composition of the graphite samples fluorinated at room temperature [23,24]. The fluorine concentration is very high, i.e. $C_{1.88}F$–$C_{1.25}F$ with some co-intercalated HF for samples R-1 and R-3. In the samples R-1 to R-3, obtained by K_2NiF_6 and elemental fluorine, very weak diffraction lines indicating the presence of NiF_2 were observed. The samples R-4 and R-5, obtained by $KAgF_4$ and elemental fluorine, contained a small amount of AgF_2 (Ag: 1–3 wt.%), hence the composition of C_xF listed in Table 1 was calculated by taking into account the amounts of fluorine bonded to AgF_2. XRD data showed that samples R-1 and R-3 were mixtures of stages 1, 2 and 3, while samples R-2, R-4 and R-5 were stage 1 compounds. The repeat distances along the c-axis (I_c) of the stage 1 phases were in the range of 0.63–0.65 nm, which is greater than the usual values of 0.50–0.60 nm. The smallest I_c-value of stage 1 C_xF is reported to be 0.47 nm [9]. In this case, fluorine atoms make a single intercalated layer between each pair of graphene layers. With increasing concentration of fluorine, their orientation changes due to close packing structure and they are transformed into double layers. This results in an expansion of fluorine-intercalated layers. As mentioned earlier, in stage 1 C_xF compounds, semi-covalent C–F bonds are formed and hence there is an increase in C–C bond length (or a_0) with respect to original graphite. In the

Table 2
Composition of C_xF samples prepared by elemental fluorine at 380 °C

Sample	Fluorination time	Composition
L-1	1 h	$C_{18.18}F$
L-2	2 h	$C_{16.94}F$
L-3	14 h	$C_{2.90}F$
L-4	1 day	$C_{2.24}F$
L-5	4 days	$C_{1.82}F$
L-6	5 days	$C_{1.56}F$
L-7	1 week	$C_{1.57}F$
L-8	2 weeks	$C_{1.51}F$

Table 3
Composition of C_xF samples prepared by elemental fluorine at 515 °C

Sample	Fluorination time (min)	Composition	Color
H-1	1	$C_{1.90}F$	Black
H-2	2	$C_{1.45}F$	Black-brown
H-3	3	$C_{1.27}F$	Brown
H-4	15	$C_{1.21}F$	Gray-brown
H-5	30	$C_{1.19}F$	Gray
H-6	600	$C_{1.06}F$	White

present case, the lattice parameter a_0 is larger than that of graphite, being in the range of 0.2464–0.2477 nm as compared to 0.2461 nm for graphite. This indicates that the major component of the samples is highly fluorinated stage 1 phase. Because in case of stage 2 and higher stages with ionic bonding, the C–C bond length (or a_0) is shortened due to a charge transfer from graphite to intercalated fluorine as in the case of other acceptor graphite intercalation compounds. An increase in a_0 depends upon the orientation of the fluorine atoms between graphene layers as well as the C–F covalency.

Fluorination conditions and composition of the fluorinated graphite samples prepared at 380 °C are given in Table 2 [25]. The fluorine content increased with increasing fluorination time from 1 h to 2 weeks from $C_{29.06}F$ ($CF_{0.0344}$) to $C_{1.51}F$ ($CF_{0.662}$). The ideal composition of $(C_2F)_n$ is $CF_{0.5}$. But it has larger fluorine content due to the formation of a $(CF)_n$ in the surface region. Fig. 1 shows X-ray diffraction pattern of samples L-1 to L-8 [25]. For the samples fluorinated for 1 h to 4 days, a strong (0 0 2) diffraction line and very weak (0 0 4) line of graphite were observed. Apart from those, very weak (1 0 1) and (1 0 2) diffraction lines indicating graphitic stacking of graphene layers were also detected in samples L-1 to L-4. Very broad and weak diffraction (0 0 1) line of $(C_2F)_n$ appeared at 0.756 and 0.789 nm for samples L-1 and L-2, respectively. The intensity of this peak increased with increasing fluorination time and the *d*-value approached 0.85–0.87 nm corresponding to (0 0 1) diffraction line of $(C_2F)_n$ [4]. The (0 0 1) lines of $(C_2F)_n$ were strong for samples L-5 to L-8 fluorinated between 4 days and 2 weeks. The most significant feature of the samples L-5 to

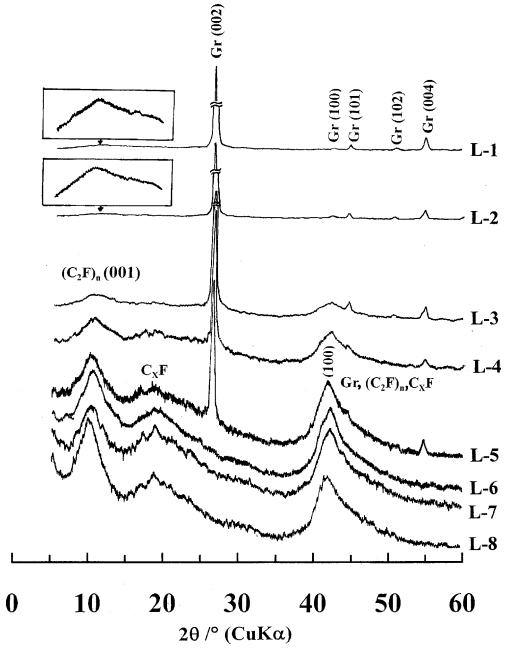

Fig. 1. X-ray diffraction patterns of graphite fluorinated at 380 °C as a function of fluorination time (sample numbers are the same as given in Table 1).

L-8 is the appearance of weak diffraction line of C_xF at 0.47 nm, indicating that an intercalated phase might have formed first leading to the formation of graphite fluoride. The existence of intercalated C_xF phase with sp^2 character could be the reason for black color of $(C_2F)_n$. The disappearance of (1 0 1) and (1 0 2) diffraction lines and increase in the intensity of (1 0 0) line show that high structural order of graphite along *a*- and *c*-axes is lost by fluorination. The a_0-values are in the range of 0.2464–0.2477 nm, which is larger than that of graphite, 0.2461 nm. This shows that the C–C bond length is increased by the formation of covalent C–F bond.

Table 3 shows the graphite fluoride samples prepared at 515 °C [24]. The composition is in the range $C_{1.90}F$–$C_{1.06}F$. The color of the samples changed from black to white with increasing time of fluorination, consequently indicating higher fluorine content. The samples fluorinated for 1–3 min (H-1 to H-3) were black to brown, while those fluorinated for 15 min or more were gray-brown to white, suggesting that these samples (H-4 to H-6) are graphite fluorides with puckered graphene layers [1–6]. The X-ray diffraction data show graphite phase for samples H-1 and H-2, but the intensity of (0 0 1) peak corresponding to $(CF)_n$ was too poor to be clearly observed due to highly disorder stacking of puckered graphene layers along the *c*-axis, because the original graphite was a fine powder with average particle size of 7 μm.

The nature of C–F bonding in all three types of graphite fluorides was analyzed by infrared (IR) absorption spectroscopy. The data are shown in Fig. 2 for samples R-5, L-7 and H-5. Other spectra are similar to those shown in Fig. 2. Sample R-5 shows multiple absorption peaks. The main vibration mode is at 1134 cm^{-1} corresponding to C–F semi-covalent bonding with weak absorption bands at 1196, 1231 and 1256 cm^{-1} probably due to nearly covalent and covalent C–F bonds. Another absorption band at 1340 cm^{-1} is due to asymmetric stretching vibrations of $>CF_2$ groups present at the surface [4–6]. A very strong band at 1522 cm^{-1} (A_{2u} vibration mode) is due to planer graphene layer structure. Sample L-7 fluorinated at 380 °C shows a very strong vibration mode at 1220 cm^{-1} due to C–F covalent bonding [4–6]. An absorption band at 1340 cm^{-1} is due to asymmetric stretching vibrations of $>CF_2$ groups [4–6]. Absence of A_{2u} absorption mode in L-7 suggests that all the graphene layers are arranged in sp^3 type puckered structure. Sample H-5 fluorinated at 515 °C shows similar IR spectrum to that of L-7 with a very strong absorption mode at 1218 cm^{-1} with a weak absorption mode at 1341 cm^{-1}.

2.2. Raman spectra of highly fluorinated graphite samples

Fig. 3 shows Raman spectra of graphite powder and graphite samples fluorinated at room temperature. Original graphite powder shows two Raman modes at 1580 (E_{2g2}) and 1360 cm^{-1} (A_{1g}). As can be seen in Fig. 3, the original

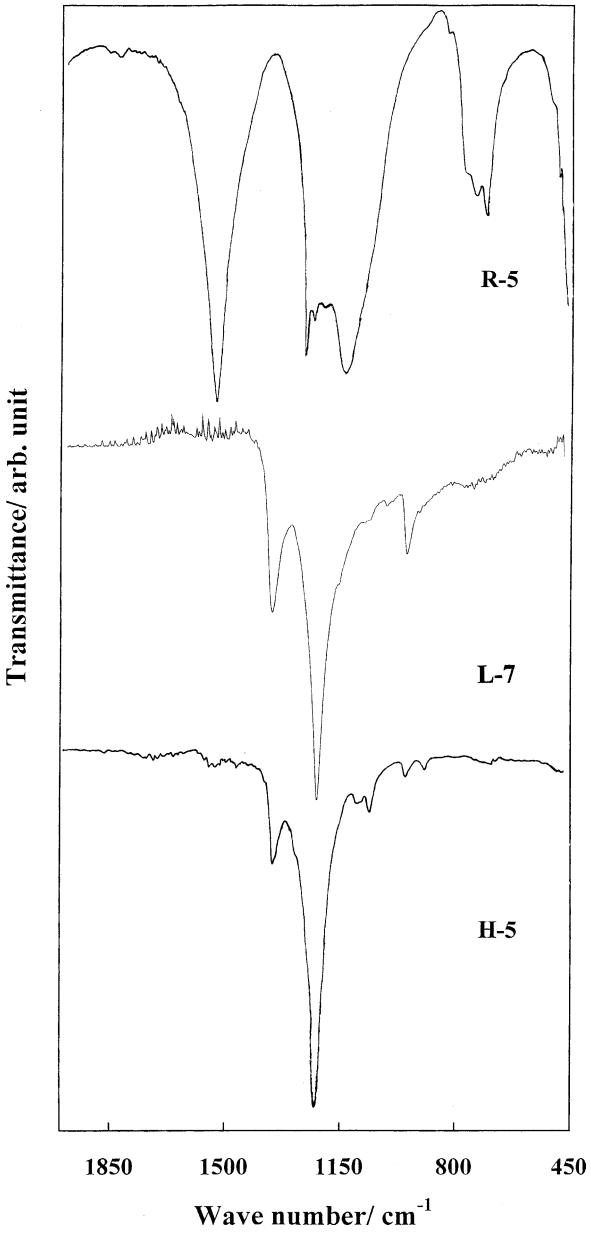

Fig. 2. IR absorption spectra of highly fluorinated graphite samples (R-5, L-7 and H-5 in Tables 1–3).

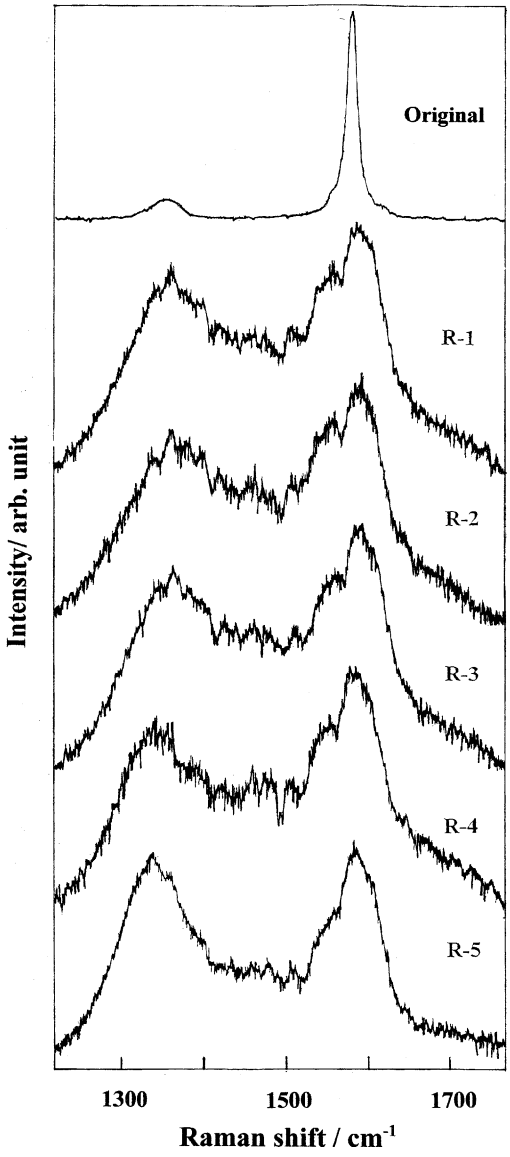

Fig. 3. Raman spectra of original graphite and those fluorinated at room temperature (sample numbers are given in Table 1).

graphite phonon mode at 1580 cm^{-1} splits into two modes after fluorination. The mode at 1593–1583 cm^{-1} is induced by charge density redistribution accompanying the contraction of C–C bond length as a result of an electron transfer from carbon to fluorine. This is a usual phenomenon observed in acceptor type graphite intercalation compounds [18–22]. A novel band is observed at 1555–1542 cm^{-1}. An increase in the C–C bond length, i.e. lattice parameter a_0 (Table 1) would bring about such a change in the Raman spectra due to the formation of C–F semi-covalent bond resulting in partial localization of charge carriers [20]. All the samples in Fig. 3 show well-ordered phonon peaks which indicate the existence of planar graphene layers in these compounds in spite of high fluorine concentration [24]. The phonon mode D at ~1360 cm^{-1} for original graphite was shifted to the range of 1356–1337 cm^{-1} for fluorinated graphite samples. The intensity was also significantly enhanced by fluorination, suggesting high disorder of the C_xF samples. The peak positions of the three Raman phonon modes shifted to lower frequencies with increasing fluorine content in C_xF, i.e. from 1593, 1555 and 1356 to 1583, 1542 and 1337 cm^{-1}, respectively. This further confirms the fact that the vibrational energy of graphene layers decreases with increase in the fluorine content of C_xF due to a weakening of the C–C bond as given in Table 1. Several weak phonon modes are observed between 1350 and 1500 cm^{-1}. Neither fluorine nor C–F bonds have vibrational energies between 1350 and 1500 cm^{-1}. Such type of phonon modes could be due to either doubling the Brillouin zone as observed by Ohana et al. [22], or disorder induced ones.

Fig. 4 shows Raman spectra of graphite fluorinated at 380 °C (Table 2) [25]. The profile of the spectra is similar to those for highly fluorinated C_xF samples though samples L-1 to L-5 contain unreacted graphite phase. Raman spectra L-1 to L-5 clearly show broad phonon bands between 1560 and 1540 cm^{-1}. This can be attributed to intercalated C_xF phase as discussed above. This indicates that structure of graphite fluorides is similar to fluorine–graphite intercalation compounds in the initial stage of fluorination. The phonon modes at 1586, 1555 and 1333 cm^{-1} for 1 h fluorination (Fig. 4, L-1) shift to 1579, 1542 and 1324 cm^{-1} phonon frequencies for sample L-5. The intensity of G band derived of graphite decreases with increasing fluorination time. According to the decrease in G band intensity, the relative intensity of D band increased. Further fluorination leads to complete conversion of graphite skeleton from sp^2 to sp^3 type structure. The spectrum L-7 in Fig. 4 was obtained for 1 week-fluorinated sample, which gave no Raman shifts because the sample was graphite fluoride, $(C_2F)_n$ with a trace of intercalated C_xF phase. The 5 days- and 2 weeks-fluorinated samples showed almost the same Raman spectra as that of sample L-7.

Fig. 5 shows Raman spectra of C_xF samples prepared at 515 °C [24]. Interestingly, samples H-1 and H-2 prepared at 515 °C also show similar Raman spectra to those of C_xF samples prepared at room temperature. This is in agreement with the fact that graphene layers keep the planarity in the fluorinated phases. Raman spectrum of sample H-3 shows that graphite skeleton is not completely destroyed by fluorine, but the process is in the transition stage. The samples fluorinated for 1–3 min (H-1 to H-3) were black to brown, while those fluorinated for 15 min or more were gray-brown

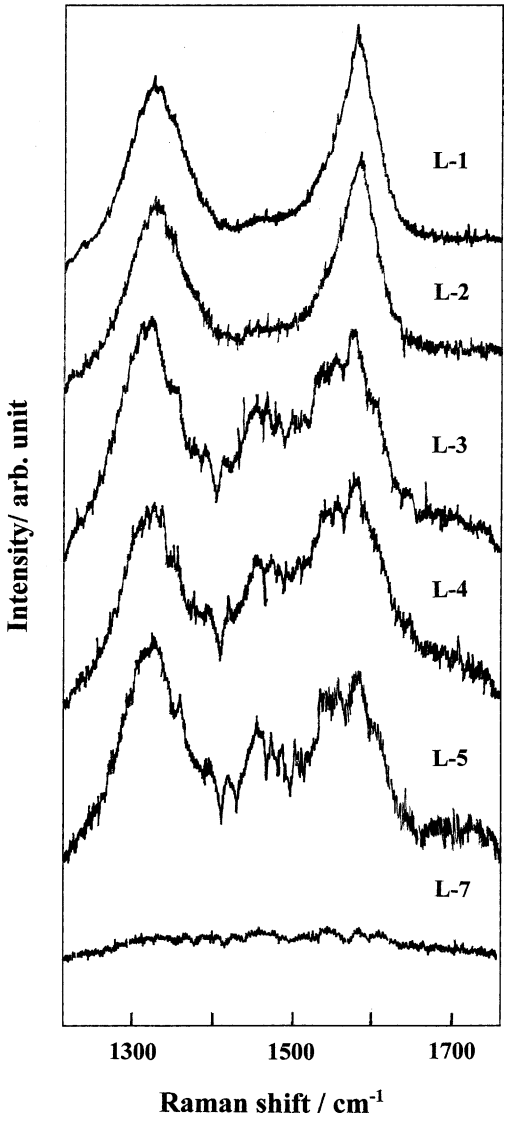

Fig. 4. Raman spectra of graphite samples fluorinated at 380 °C (sample numbers are given in Table 2).

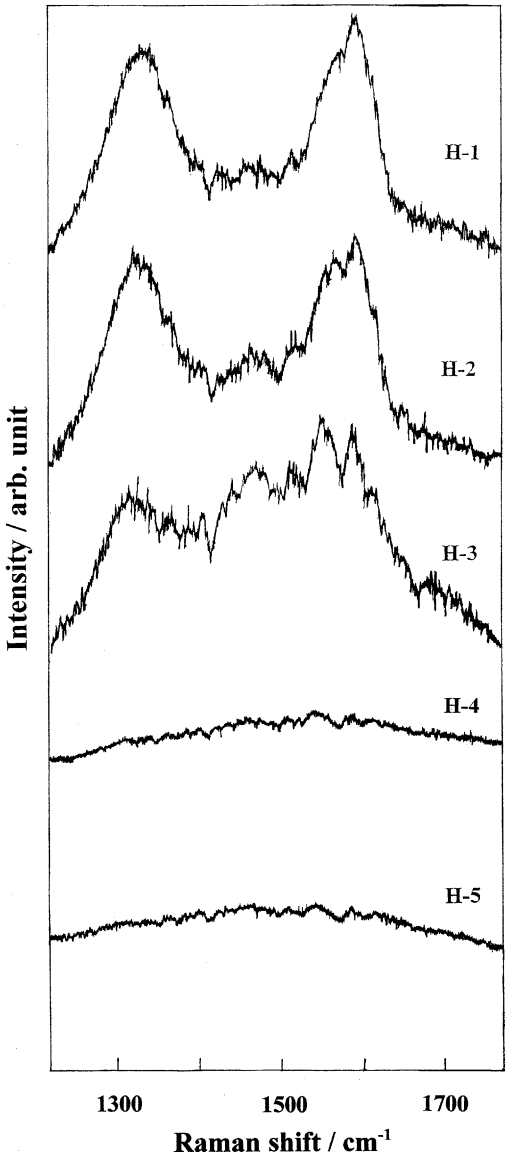

Fig. 5. Raman spectra of graphite samples fluorinated at 515 °C (sample numbers are given in Table 3).

to white, suggesting that these samples (H-4 to H-6) are graphite fluorides with puckered graphene layers. For samples H-4 to H-6 prepared for 15 min or more, all Raman modes completely disappeared due to the high level of disorder. Change of graphene layer from sp^2 to sp^3 hybridization breaks the translation symmetry of the planar graphene layers and relaxes the conservation law of wave vector. So all phonon modes in principle can contribute to the Raman scattering process. Consequently, usual Raman active phonon modes in the Brillouin zone is replaced by multiple Raman active phonons at the center of the mini-zone. The change of the Raman spectrum profile with fluorination time shown here schematically depict the change of graphene layers from sp^2 to sp^3 hybridization accompanying the color change, that is, the planar graphene layer is changed to a cyclohexane chair.

The Raman phonon peaks of G and D bands for graphite samples fluorinated at room temperature, 380 and 515 °C are plotted in Fig. 6a and b, respectively, along with the previously reported data. It is obvious from Fig. 6 that the peak phonon modes occurring in all types of C_xF show a general trend with a sharp anomalous downshift at around C_2F due to the change in C–F bonding from the semi-covalent to covalent [24]. This reduction is larger in the D band for samples prepared at 515 °C because samples H-1 to H-5 are more strongly fluorinated.

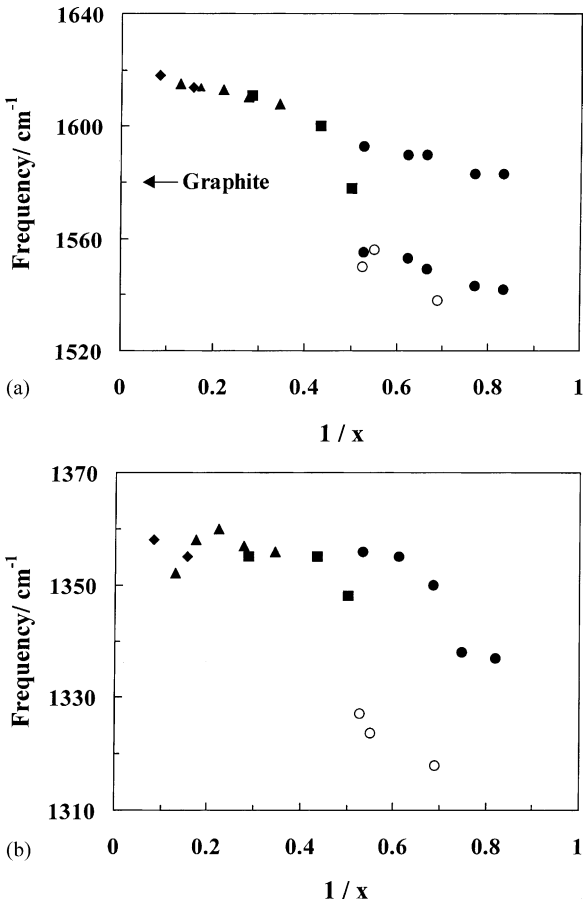

Fig. 6. Raman shifts as a function of $1/x$ in C_xF: (■) [19], (▲) [20], (◆) [22], (●) this work (obtained at room temperature), (○) this work (obtained at (a) 380 and (b) 515 °C for $1 < x < 2$ in C_xF).

The Raman spectra shown in Figs. 3–5 reveal the intermediate stages leading to the formation of graphite fluoride at high temperatures. This is schematically shown in Fig. 7. In the beginning of fluorination, fluorinated graphite phase keeps the planarity of graphene layers with ionic and semi-covalent C–F bonds (Fig. 7b and c). As shown in Fig. 1, stage 1 C_xF phase was detected in graphite fluorinated at 380 °C. Since stage 2 and higher stage compounds are not stable as the stage 1, their detection may be difficult even if they exist in the intermediate state of fluorination. The reaction rate is relatively slower at 380 than 515 °C. Therefore, fluorinated graphite can take a lower entropy structure such as $(C_2F)_n$ with doubly puckered graphene layers [4–6]. The formation of doubly puckered graphene layers of $(C_2F)_n$ from stage 1 C_xF phase may be understood by Daumas–Hérold staging model [18] because fluorine atom is mobile between graphene layers even at stage 1 [5] (Fig. 7e). On the other hand, the reaction rate is much higher at 515 than 380 °C. Thus, a higher entropy structure such as $(CF)_n$ is preferable at 515 °C. At this temperature, stage 1 C_xF phase is easily converted to $(CF)_n$ with singly puckered graphene layers (Fig. 7d).

3. Conclusion

Fluorination process of graphite at high temperatures has been investigated. Graphite samples fluorinated at 380 °C for 1 h to 4 days and at 515 °C for 1–3 min demonstrate the same Raman spectra as those of highly fluorinated graphite samples prepared at room temperature using K_2NiF_6 or $KAgF_4$ and elemental fluorine. This indicates that the fluorinated phase still keeps the planarity of graphene layers in the intermediate state even at high temperatures. X-ray diffraction patterns of graphite samples fluorinated at 380 °C also show the existence of stage 1 C_xF phase with planar graphene layers. These data strongly suggest that graphite fluorides, $(CF)_n$ and $(C_2F)_n$ with puckered graphene layers are formed through the stage 1 C_xF phase at high temperatures. The formation of $(C_2F)_n$ with doubly puckered graphene layers can be understood by Daumas–Hérold staging model because intercalated fluorine atom is mobile in stage 1 C_xF.

4. Experimental

4.1. Synthesis of highly fluorinated graphite samples at room temperature, 380 and 515 °C

For the preparation of highly fluorinated graphite samples at room temperature, natural graphite powder (Madagascar, particle size: 57–74 μm, purity: 99.4%) was fluorinated by

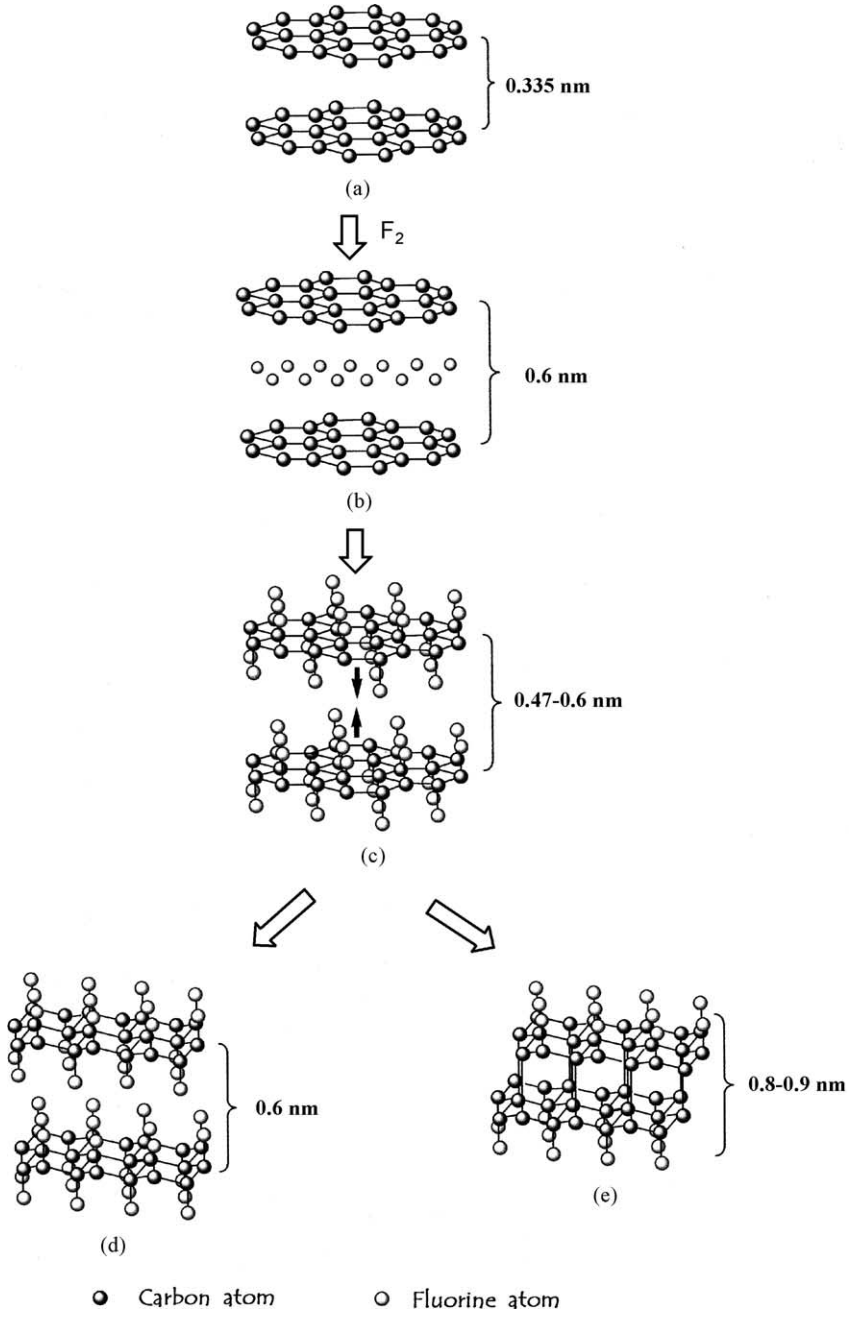

Fig. 7. Schematic representation of formation mechanism of graphite fluoride at high temperatures: (a) graphite; (b) intermediate C_xF phase with ionic C–F bonds; (c) intermediate C_xF phase with semi-covalent C–F bonds; (d) graphite fluoride, $(CF)_n$; (e) graphite fluoride, $(C_2F)_n$.

K_2NiF_6 or $KAgF_4$ and elemental fluorine under pressure (7.9–11.8) $\times$ 10^5 Pa in anhydrous HF (aHF). The prepared C_xF samples were contaminated with by-products insoluble in aHF, either NiF_2 or AgF_2. To remove these impurities, the prepared C_xF samples were treated by AsF_5 in order to obtain products very soluble in aHF, $Ni(AsF_6)_2$ or $Ag(AsF_6)_2$. The details of the experimental procedure are described in a previous paper [23]. Natural graphite powder (Madagascar, particle size: 57–74 μm, purity: 99.4%) was fluorinated at 380 °C by 1.0 $\times$ 10^5 Pa F_2 for 1 h to 2 weeks using a batch type nickel reactor. Fluorination of natural graphite powder (average particle size: 7 μm) was also performed at 515 °C by 1.0 $\times$ 10^5 Pa F_2 for 1 min to 10 h.

4.2. Analyses of the products

The fluorinated graphite samples were analyzed by elemental analysis of carbon, hydrogen and fluorine at the Elemental Analysis Center of the Faculty of Pharmaceutical Science of Kyoto University. Raman spectroscopy (Jobin-Yvon T-64000 with Ar ion laser of 514.5 nm), IR absorption spectroscopy (Perkin-Elmer 2000, KBr disk method) and

X-ray diffractometry (Shimadzu XD-610 with Cu Kα radiation) were applied to the characterization of fluorinated graphite samples. The small amounts of silver contained in samples R-4 and R-5 in Table 1 were analyzed at Jožef Stefan Institute as follows. The sample was hydrolyzed in HNO_3 solution and heated on a sand bath for 2 h with further addition of HNO_3. After filtration, the amount of silver in the filtrate was determined by atomic absorption spectroscopy. The amount of silver in the solid residue was also obtained by atomic absorption spectroscopy after decomposition of the solid residue in a melt of $KNaCO_3$.

References

[1] O. Ruff, O. Bretschneider, Z. Anorg. Allg. Chem. 217 (1934) 1–18.
[2] W. Rüdorff, G. Rüdorff, Chem. Ber. 80 (1947) 417–423.
[3] Y. Kita, N. Watanabe, Y. Fujii, J. Am. Chem. Soc. 101 (1979) 3832–3841.
[4] N. Watanabe, T. Nakajima, H. Touhara, Graphite Fluorides, Elsevier, Amsterdam, 1988.
[5] T. Nakajima, N. Watanabe, Graphite Fluorides and Carbon–Fluorine Compounds, CRC Press, Boca Raton, 1991.
[6] T. Nakajima, Synthesis, structure, and physicochemical properties of fluorine–graphite intercalation compounds, in: T. Nakajima (Ed.), Fluorine–Carbon and Fluoride Carbon Materials, Marcel Dekker, New York, 1995, pp. 1–32.
[7] T. Nakajima, Fluorinated carbon materials for energy conversion, in: T. Nakajima, B. Žemva, A. Tressaud (Eds.), Advanced Inorganic Fluorides, Elsevier, Amsterdam, 2000, pp. 493–520.
[8] T. Mallouk, N. Bartlett, J. Chem. Soc., Chem. Commun. (1983) 103–104.
[9] R. Hagiwara, M. Lerner, N. Bartlett, J. Chem. Soc., Chem. Commun. (1989) 573–574.
[10] H. Touhara, K. Kadono, Y. Fujii, N. Watanabe, Z. Anorg. Allg. Chem. 544 (1987) 7–20.
[11] A. Tressaud, V. Gupta, L. Piraux, L. Lozano, E. Marquestaut, S. Flandrois, A. Marchand, O.P. Bahl, Carbon 32 (1994) 1485–1492.
[12] V. Gupta, R.B. Mathur, O.P. Bahl, A. Tressaud, S. Flandrois, Synth. Met. 73 (1995) 69–75.
[13] A. Tressaud, M. Chambon, V. Gupta, S. Flandrois, O.P. Bahl, Carbon 33 (1995) 1339–1345.
[14] R.B. Mathur, V. Gupta, O.P. Bahl, A. Tressaud, S. Flandrois, Synth. Met. 114 (2000) 197–200.
[15] A. Tressaud, C. Guimon, V. Gupta, F. Moguet, Mater. Sci. Eng. B30 (1995) 61–68.
[16] F. Tuinstra, J.L. Koenig, J. Chem. Phys. 53 (1970) 1126–1130.
[17] D.S. Knight, W.B. White, J. Mater. Res. 4 (1989) 385–393.
[18] M.S. Dresselhaus, G. Dresselhaus, Adv. Phys. 30 (1981) 139–326.
[19] T. Mallouk, B.L. Hawkins, M.P. Conrad, K. Zilm, G.E. Maciel, N. Bartlett, Phil. Trans. R. Soc. London Ser. A 314 (1985) 179–187.
[20] A.M. Rao, A.W.P. Fung, S.L. Vittorio, M.S. Dresselhaus, G. Dresselhaus, M. Endo, K. Oshida, T. Nakajima, Phys. Rev. B 45 (1992) 6883–6891.
[21] M.S. Dresselhaus, M. Endo, J.P. Issi, Physical properties of fluorine and fluoride–graphite intercalation compounds, in: T. Nakajima (Ed.), Fluorine–Carbon and Fluoride Carbon Materials, Marcel Dekker, New York, 1995, pp. 95–186.
[22] I. Ohana, I. Palchan, Y. Yacoby, D. Davidov, H. Selig, Solid State Commun. 56 (1985) 505–508.
[23] T. Nakajima, M. Koh, V. Gupta, B. Žemva, K. Lutar, Electrochim. Acta 45 (2000) 1655–1661.
[24] V. Gupta, T. Nakajima, B. Žemva, J. Fluorine Chem. 110 (2001) 145–151.
[25] V. Gupta, T. Nakajima, Y. Ohzawa, Collect. Czech. Chem. Commun. 67 (2002) 1366–1372.